

RESEARCH LETTER

10.1002/2015GL067124

Key Points:

- The role of regional aerosol forcing on East Asian summer monsoon
- Modeling experiments for aerosol forcing
- Different role of SST and aerosol forcings

Supporting Information:

- Figures S1–S6 and Tables S1 and S2

Correspondence to:

S.-W. Yeh and R. J. Park,
 swyeh@hanyang.ac.kr;
 rjpark@snu.ac.kr

Citation:

Kim, M. J., S.-W. Yeh, and R. J. Park (2016), Effects of sulfate aerosol forcing on East Asian summer monsoon for 1985–2010, *Geophys. Res. Lett.*, *43*, 1364–1372, doi:10.1002/2015GL067124.

Received 21 NOV 2015

Accepted 8 JAN 2016

Accepted article online 9 JAN 2016

Published online 9 FEB 2016

©2016. American Geophysical Union.

All Rights Reserved.

This is an open access article under the terms of the Creative Commons Attribution-NonCommercial-NoDerivs License, which permits use and distribution in any medium, provided the original work is properly cited, the use is non-commercial and no modifications or adaptations are made.

Effects of sulfate aerosol forcing on East Asian summer monsoon for 1985–2010

Minjoong J. Kim¹, Sang-Wook Yeh², and Rokjin J. Park¹

¹School of Earth and Environmental Sciences, Seoul National University, Seoul, Korea, ²Department of Marine Sciences and Convergent Technology, Hanyang University, Ansan, Korea

Abstract We examine the effect of anthropogenic aerosol forcing on the East Asian summer monsoon (EASM) using the Community Atmosphere Model version 5.1.1. One control and two sensitivity model experiments were conducted in order to diagnose the separate roles played by sea surface temperature (SST) variations and anthropogenic sulfate aerosol forcing changes in East Asia. We find that the SST variation has been a major driver for the observed weakening of the EASM, whereas the effect of the anthropogenic aerosol forcing has been opposite and has slightly intensified the EASM over the recent decades. The reinforcement of the EASM results from radiative cooling by the sulfate aerosol forcing, which decelerates the jet stream around the jet's exit region. Subsequently, the secondary circulation induced by such a change in the jet stream leads to the increase in precipitation around 18–23°N. This result indicates that the increase in anthropogenic emissions over East Asia may play a role in compensating for the weakening of the EASM caused by the SST forcing.

1. Introduction

Monsoons play a key role in global mass and heat transport [Trenberth *et al.*, 2000]. In particular, the East Asian monsoon system is one of the strong global monsoon systems caused by the large thermal contrast between the Asian continent and the Pacific Ocean [Wang and Ding, 2006]. This system includes both the subtropics and the midlatitudes, and its concentrated rain belts stretch for many thousands of kilometers, affecting China, Japan, Korea, and the surrounding areas [Wang *et al.*, 2001].

The previous studies suggested that the East Asian summer monsoon system is primarily influenced by sea surface temperature (SST) forcings including El Niño–Southern Oscillation, the western Pacific SST, and those of the surrounding oceans [Wang *et al.*, 2004, and references therein]. However, recent studies have argued that increased aerosol forcing can also change the monsoon system over East Asia [Liu *et al.*, 2009] by affecting clouds and precipitation through direct and indirect effects [Albrecht, 1989; Haywood and Boucher, 2000; Twomey, 1977]. The rapid industrialization of Asia has caused dramatic increases of primary aerosol and aerosol precursor emissions over the past half century [Smith *et al.*, 2011]. The enhancement in aerosol concentration induces atmospheric cooling and suppresses monsoon circulation, resulting in a weakening of monsoon strength with a decreased precipitation over Asia over the past decades [Kim *et al.*, 2007; Bollasina *et al.*, 2011; Cowan and Cai, 2011; Ganguly *et al.*, 2012; Bollasina *et al.*, 2014].

Recent modeling studies with more sophisticated physics, however, have drawn contentious conclusions regarding the impact of aerosols on the East Asian monsoon system. Guo *et al.* [2013] showed that the strength of East Asian monsoon has weakened due to the sulfate aerosol forcing in the postmonsoon season, although the strength of East Asian monsoon has not significantly changed at the 95% significance level during which anthropogenic sulfate aerosol has increased in boreal summer. Jiang *et al.* [2013] showed Community Atmosphere Model version 5.1.1 (CAM5) simulations that sulfate aerosol plays a role in enhancing the monsoonal circulation and precipitation over the South China Sea and the western Pacific Ocean. Bollasina *et al.* [2013] found that aerosols are likely responsible for the observed earlier Indian monsoon onset, resulting in enhanced precipitation over most of India during June. Based on Coupled Model Intercomparison Project Phase 5 (CMIP5) results, Guo *et al.*, 2015 suggested that the aerosol indirect effects are likely related to the negative rainfall trend, whereas the direct radiative effect is associated with the increase in monsoon rainfall. Turner and Annamalai [2012] concluded that the South Asian precipitation during the twentieth century cannot be explained by atmospheric CO₂ concentration and global temperature increase because of the effects of aerosols. Therefore, aerosol clearly represents a major uncertainty for the monsoon projections in the future climate.

Although the previous studies have significantly contributed to the understanding of the effects of aerosol on the East Asia summer monsoon system, it is still debatable as to whether aerosol forcing strengthens or weakens the monsoon system over East Asia [Kuhlmann and Quaas, 2010]. In this study, we revisit this issue using the extended observations and an improved model with the realistic boundary conditions (aerosol emissions) for long-term simulations in East Asia.

2. Data and Methodology

2.1. Reanalysis Data Set and Monsoon Index

We use the reanalysis data sets and the climate model simulation to quantify the contribution of anthropogenic aerosol forcing to the East Asian summer monsoon (EASM) intensity trend over the past. The data sets in our analysis below include the National Centers for Environmental Prediction (NCEP)/Department of Energy (DOE) reanalysis II (RA2) data sets [Kanamitsu *et al.*, 2002] and the Global Precipitation Climatology Project (GPCP) monthly precipitation data set version 2.2 for 1985–2010 [Adler *et al.*, 2003]. Many of the EASM indices based on atmospheric variables, such as pressure, ocean-land temperature contrast, wind field, and precipitation, have been widely used to quantify monsoon strength and variability over monsoon regions [Wang *et al.*, 2009]. In the present study, we apply the definition of the EASM index by Li and Zeng [2002] to the NCEP DOE RA2 data set, which is referred to as the observation [Nan and Li, 2003; Zhu *et al.*, 2012]. The EASM index is defined as follows:

$$\text{EASMI} = \frac{\|\bar{V}_W - V_i\|}{\|\bar{V}\|} - 2,$$

where \bar{V}_W and V_i are the reference climatological winter wind vector and monthly wind vector at point i , respectively, and $\bar{V} = (\bar{V}_W + \bar{V}_S)/2$ is the climatological mean wind vector. \bar{V}_S is the climatological summer wind (for the Northern Hemisphere, taking $\bar{V}_W = \bar{V}_{\text{Jan}}$ and $\bar{V}_S = \bar{V}_{\text{Jul}}$). The norm $\|A\|$ is defined as follows:

$$\|A\| = \left(\iint_S |A|^2 \, dS \right)^{1/2},$$

where S denotes the domain of our interest. According to Li and Zeng [2002], the domain of the EASM index is defined for 10–40°N and 110–140°E. There is an apparent negative correlation between the EASM index and rainfall variability in the middle and lower valleys of the Yangtze River in China during the boreal summer (June–July–August, JJA), indicating that drought years over the valley are associated with a strong EASM and flood years with a weak EASM [Nan and Li, 2003].

2.2. Model Simulations

We performed model simulations using the NCAR Community Atmosphere Model version 5 (CAM5) model coupled with the Community Land Surface Model version 4 [Neale *et al.*, 2012]. The CAM5 model is based on the finite volume (FV) dynamical core at a 1.9°×2.5° horizontal resolution and with 30 vertical levels. For this study, the ocean and ice modules were not fully coupled but were communicated to the atmosphere via an oceanic surface boundary condition, given as midmonth values of sea surface temperature, as well as sea ice fractions over the polar region. The sea surface temperature and the sea ice fractions are time series data constructed by concatenating and interpolating global HadISST data from the Met Office Hadley Center [Rayner *et al.*, 2003] to the FV core grids of the CAM5. For aerosol simulations, the CAM5 uses a three-mode version of the modal aerosol model (MAM3) [Liu *et al.*, 2012].

To examine the role of sulfate aerosol forcing in East Asia, we updated the Asian anthropogenic SO₂ emissions in the CAM5 with the gridded inventory for 2000 over the Asian domain (60°E–158°E and 13°S–54°N) [Streets *et al.*, 2003]. The Asian emission of SO₂ for the year 2000 was 18.9 Tg S yr⁻¹. We applied the annual scale factors of the Regional Emission inventory in Asia [Ohara *et al.*, 2007] for 1985–2010 to the Streets *et al.* [2003] emissions in order to impose interannual variations in the model. The emission of SO₂ had continuously increased until 2006 and then has slightly decreased in East Asia. The SO₂ emission in 2006 was 84% higher than that in 1985. While the SO₂ emissions in other regions are fixed following Liu *et al.* [2012], the aerosol concentration in other regions may not be constant because it can be transported from one region to the others. Because MAM3 module is fully coupled with cloud physics and radiation code, CAM5

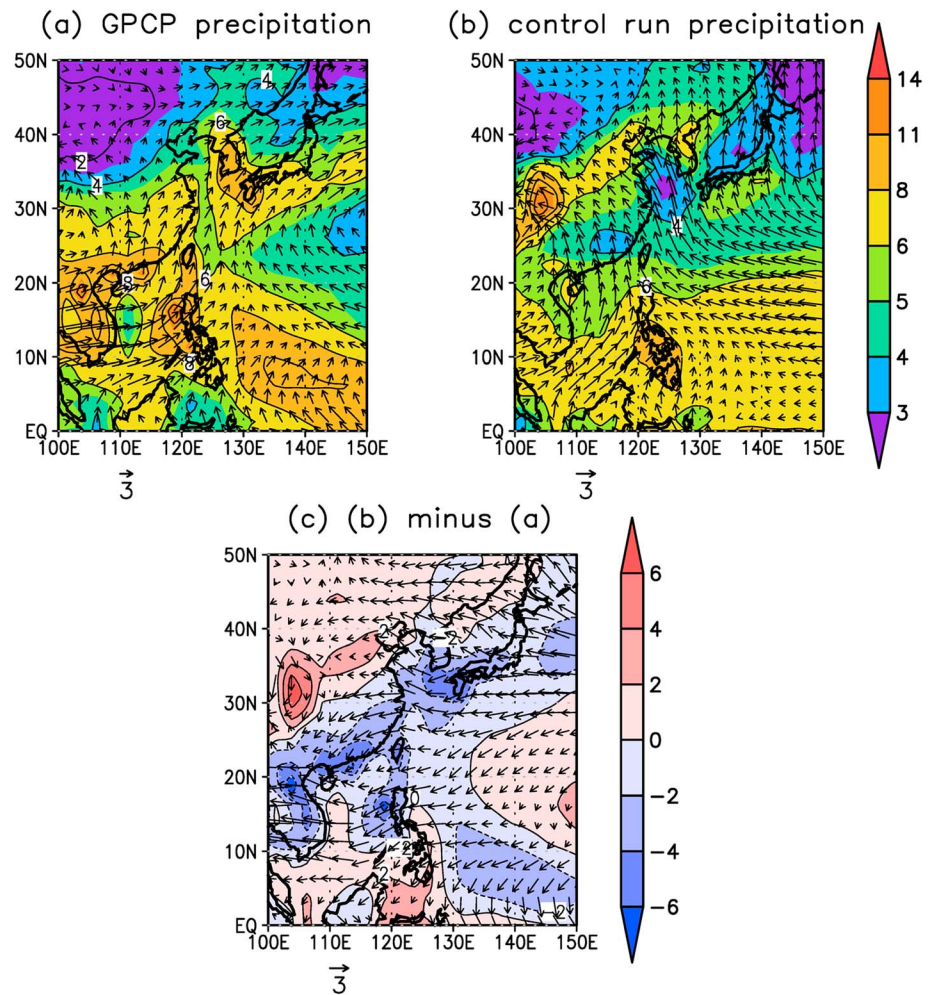


Figure 1. (a) Boreal summer mean GPCP precipitation (shaded) and NCEP DOE RA2 wind fields at 850 hPa (vector) for 1985–2010. (b) Same as Figure 1a but for the CAM5 results (control run). (c) Difference between simulated and observed results. Unit in precipitation and wind is mm d^{-1} , and m s^{-1} , respectively.

accounts for both aerosol direct and indirect effects with Asian sulfate aerosol change over the recent decades [Neale *et al.*, 2012].

We conducted three sets of model experiments using the CAM5. The first set used the historical SST for 1985–2010 with the time-varying SO_2 emissions in East Asia, hereafter referred to as the control run. The second set used the historical SST without the East Asian SO_2 emissions, which will be referred to as the SST run. Finally, the third set included the climatological SST with the time-varying SO_2 emissions in East Asia, which will be referred to as the SO_2 run. Each set of experiments was performed with four ensemble members, the average of which is presented in this study. In this study, we mainly focused on the effect of sulfate aerosol on EASM because the concentration of sulfate aerosol has dramatically increased in East Asia during the past few decades relative to those of other aerosol species such as brown and black carbon aerosols [Streets *et al.*, 2003; Li *et al.*, 2013].

3. Results

We first compare the observed mean precipitation and low-level (850 hPa) winds during JJA with the simulated values from the control run for 1985–2010 (Figures 1a and 1b). The GPCP precipitation is the highest around the Philippines and Northern Mariana Islands. The second peak is located around southern China, Japan, and Korea, and is associated with the Baiu/Meiyu/Changma front [Wang *et al.*, 2004]. On the other hand, the observed wind shows clear cyclonic circulation over southern Asia and southern China along with the southwesterlies from the ocean onto the land and anticyclonic circulation over the western North Pacific.

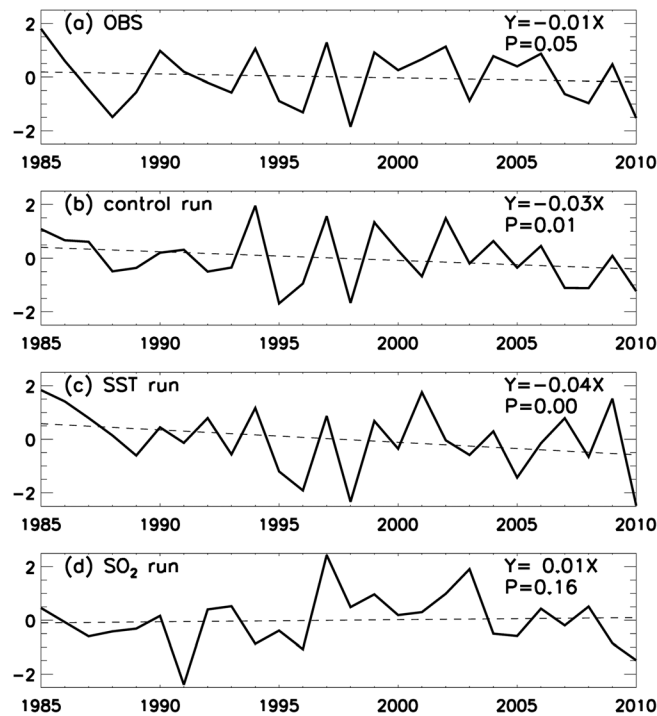


Figure 2. Time series of the EASM index from (a) the NCEP DOE RA2, (b) the control run, (c) the SST run, and (d) the SO₂ run.

The control run captures the general patterns of the observed mean precipitation and low-level winds during JJA. In particular, the model reproduced the observed precipitation band from southwestern China to the Korean peninsula. However, considerable discrepancies still exist in the detailed structures between the control run and the observation (Figure 1c), indicating the model inability of precipitation simulation, which are likely caused by our limited scientific understanding as well as simulation capability for subgrid scale processes. The overall amount of precipitation and the strength of circulation simulated in the control run are smaller and weaker than those in the observations, respectively. In addition, the magnitude of the precipitation band from southwestern China to the Korean peninsula is smaller than that of observation and its position is shifted to the north in the control run (Figure 1c). Such model biases are also found in most of the CMIP3 and CMIP5

model participants [Sperber *et al.*, 2013]. In spite of this difference, the spatial pattern in the precipitation variability associated with the EASM index in the control run is not much influenced by such discrepancies compared to the observation (see Figure S1 in the supporting information). In addition, the pattern correlation in the mean precipitation structure between the observation and the control run is 0.61 with the 95% statistical significance. Note that it is also found that the pattern correlation coefficient of each member in the control run is similar to that of the ensemble mean (Figure S2 and Table S1). Furthermore, the precipitations and winds fields in the SST run and the SO₂ run are also comparable with the control run (Figure S3).

To examine the variability in the EASM, we calculate the EASM index in the observation, the control run, the SST run, and the SO₂ run for 1985–2010 (Figures 2a–2d). Similar to many previous studies, the variability in the EASM is prominent on interannual timescales in the observation [Shi and Zhu, 1996; Wang *et al.*, 2008; Zhu *et al.*, 2005]. In addition, it is evident that the EASM index is characterized by a slight decreasing trend in the observation (Figure 2a). Such a weakening of the EASM is also found in both the control run and the SST run (Figures 2b and 2c), indicating that the overall variability in the EASM is reasonably simulated in the control run and the SST run. It should be noted that the decreasing trends in the control run and the SST run are also statistically significant at the 95% confidence level. Therefore, the EASM index in the observation is highly correlated with those in the control run and the SST run (see Table 1).

The EASM index simulated in the SO₂ run is characterized by a slightly increasing trend for 1985–2010, although the change is not statistically significant (Figure 2d). This result is in contrast to the observations and the two other runs (control run and the SST run), and it leads to negligible correlation coefficients of EASM indices between the SO₂ run and the others (Table 1). We argue that the contribution of sulfate aerosol

trend acts to strengthen the EASM during recent decades, unlike SST forcing. In other words, the weakening of the EASM in recent decades is primarily due to SST forcing. A simple comparison of the trends of the EASM index in the three runs also

Table 1. Correlations Between the EASM of the NCEP DOE RA2 and That of the Control Run, the SST Run, and the SO₂ Run Without the Trend

	Control Run	SST Run	SO ₂ Run
NCEP DOE RA2	0.52	0.45	0.10
Control run	-	0.54	0.06

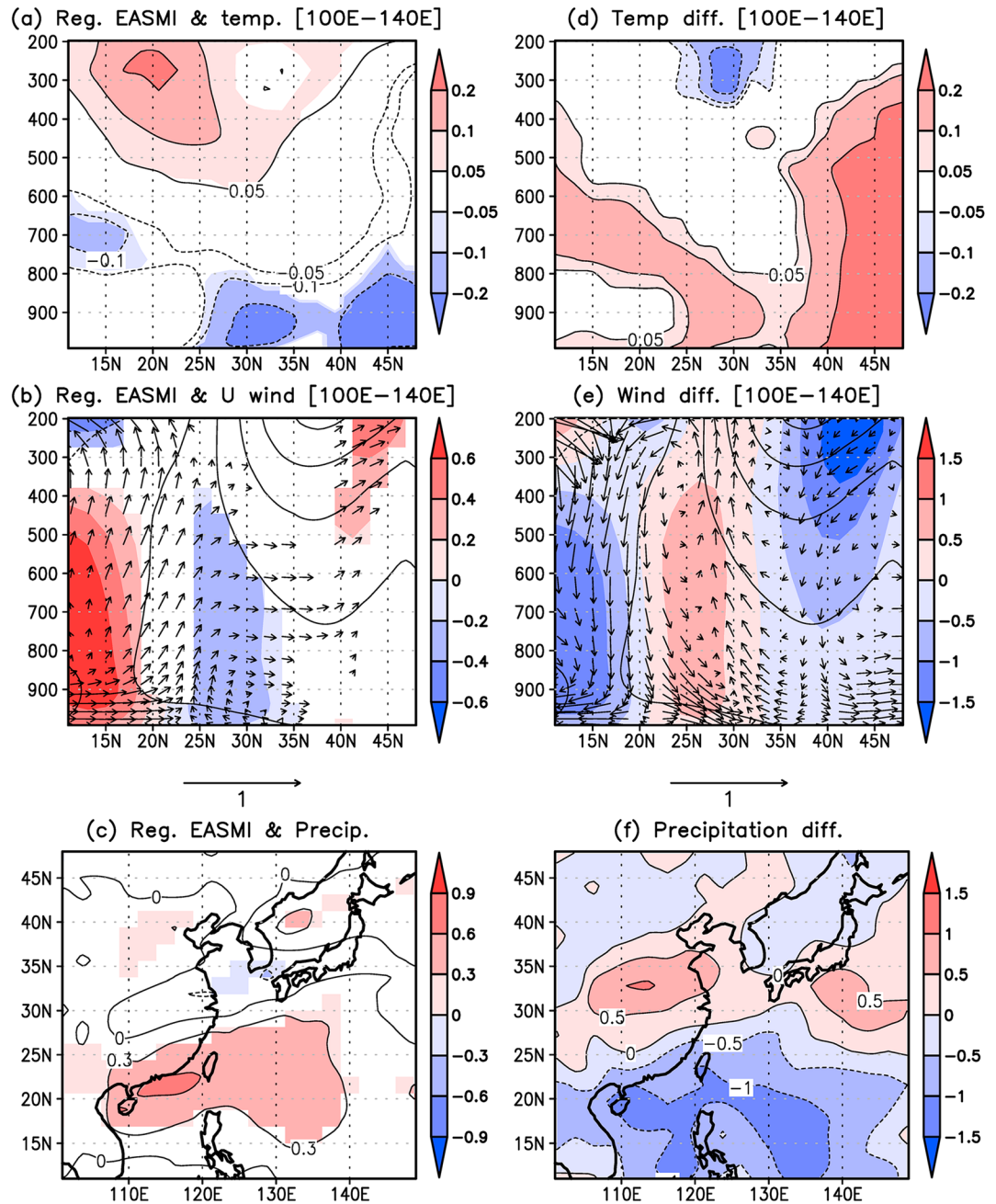


Figure 3. (a) Zonally averaged regression of temperature against the EASM index from the SST run (100°E–140°E). (b) Zonally averaged regression of wind field against the EASM index (shade = zonal wind, vector = v ; $\omega \times -30$). The solid line indicates the averaged zonal wind (1985–2010, contour interval = 5). (c) Regression of precipitation against the EASM index. Shaded denotes the statistical significance at the 95% confidence level. The differences in (d) zonally averaged temperature, (e) zonally averaged wind, and (f) precipitation between the two periods (2001–2010 minus 1985–1994) in the SST run. Units are K, $m s^{-1}$, $mm d^{-1}$, K, $m s^{-1}$, and $mm d^{-1}$, respectively.

supports this result. That is, the negative trend of the EASM index in the SST run ($-0.04 yr^{-1}$) is slightly stronger than that of the control run ($-0.03 yr^{-1}$) owing to the effect of sulfate aerosol forcing, which strengthens the EASM in the control run. Therefore, the increase in sulfate aerosol concentration over East Asia lessens the negative trend of the EASM in the control run relative to that of the SST run. It should be noted that when the first three years are removed, the observed trend of EASM becomes smaller ($-0.002 yr^{-1}$ for 1988–2010) and the trend of EASM in each member is comparable with the ensemble mean (Table S2). The simulated trends of

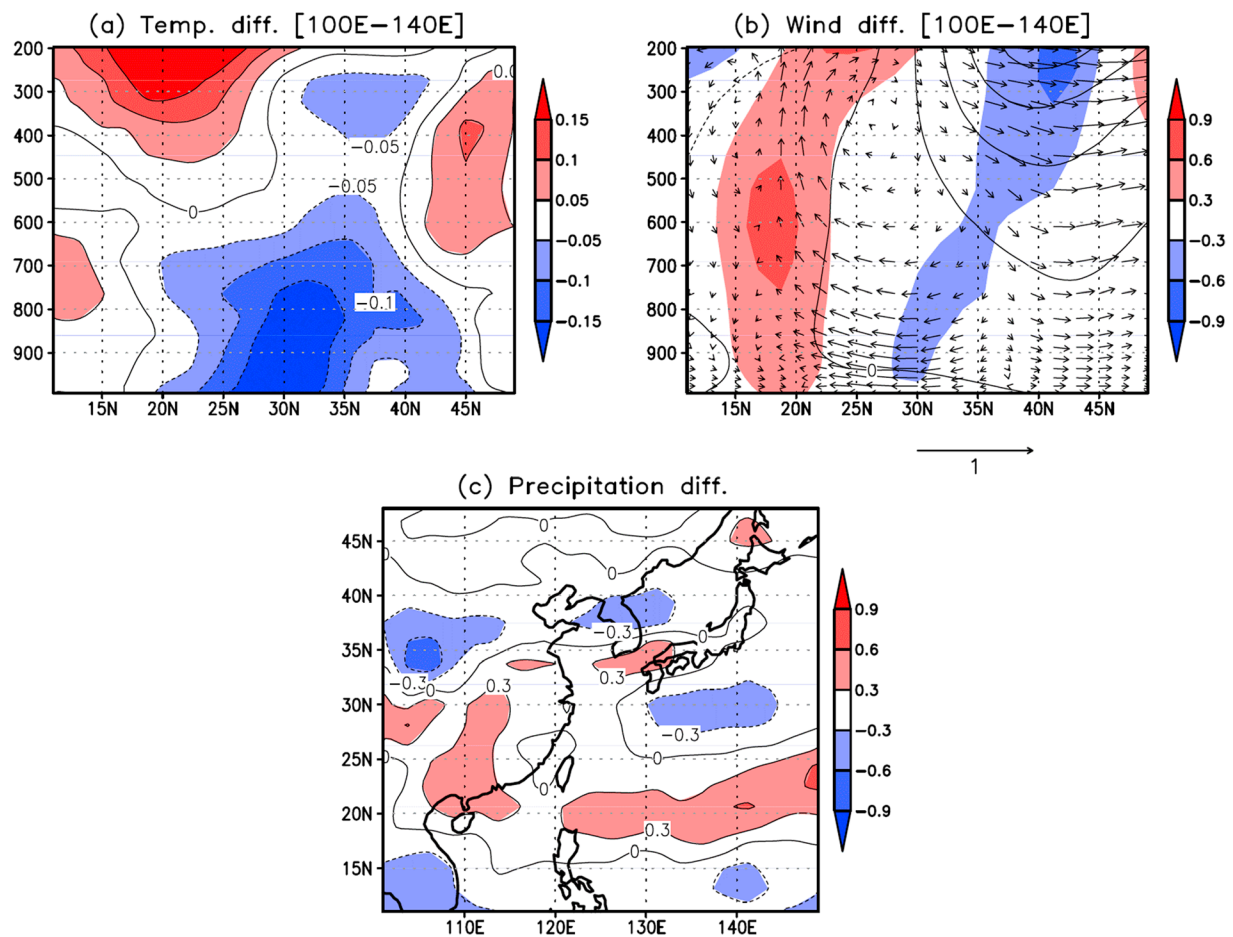


Figure 4. Differences in (a) temperature averaged over 100°E–140°E, (b) zonal wind (shading) and meridional circulation (vector = v ; $\omega \times -30$) averaged over 100°E–140°E, and (c) surface precipitation between the two periods (2001–2010 minus 1985–1994) in the SO₂ run. Units are K, K, m s^{-1} , and mm d^{-1} , respectively. The solid line in Figure 4b indicates the averaged zonal wind (1985–2010, contour interval = 5).

the control run, SST run, and SO₂ run are also similarly reduced when the first three years are removed (-0.01 yr^{-1} , -0.02 yr^{-1} , and 0.01 yr^{-1}) in the analysis. Despite of the smaller trends of the EASM both in the observation and simulations, however, the overall tendency does not change and is consistent with the results including the first three years.

We investigate the opposite roles of the SST forcing and the sulfate aerosol forcing in modulating the intensity of the EASM by comparing the SST run with the SO₂ run. We first calculate the regressed temperature against the EASM index in the SST run (Figure 3a). The regressed temperature at the upper troposphere is characterized by a warming (cooling) south (north) 40°N, which reflects an upper tropospheric condition during a strong EASM, as suggested by a previous study [Yu *et al.*, 2004]. An enhancement of the meridional temperature gradient in East Asia leads to the northward shift of the jet stream, as shown in Figure 3b. Subsequently, the northward shift of the jet stream drives the secondary circulation over East Asia, causing an increase in precipitation in East Asia (Figure 3c).

In order to understand why the EASM becomes weaker in recent decades in the SST run, we examine the differences in temperature and zonal wind at 300 hPa between 2001–2010 and 1985–1994 (2001–2010 minus 1985–1994) in the SST run. We found that the meridional temperature gradient had weakened for 2001–2010 (Figure 3d). As a result, the southward shift of the jet stream had occurred from 1985–1994 to 2001–2010, causing a decrease in precipitation in East Asia (Figure 3e). This result implies that the observed weakening of the EASM is primarily explained by SST forcing. It should be noted that similar dynamic processes are found in the control run (not shown). In addition, the regressed temperature, wind, and precipitation against the EASM index in the SO₂ run are displayed in the supporting information (Figure S4). It is found that the overall

structures in the regressed temperature, wind, and precipitation against with the EASM index are similar to that in the SST run, reflecting that the dynamical processes associated with a strong EASM are the same in the SST run and the SO₂ run, respectively.

To estimate the effects of sulfate aerosol forcing in the SO₂ run for recent decades, the change in tropospheric temperature between the two periods (2001–2010 minus 1985–1994) in the SO₂ run is displayed in Figure 4a. The increase of sulfate aerosol concentrations causes cooling in southeastern China, reflecting the thermal response due to either direct or indirect forcings of sulfate aerosol. We find, however, that the simulated changes of cloud fraction and cloud radiative forcing in the SO₂ run are relatively small between the two periods (Figures S5a and S5b in the supporting information), indicating that the simulated indirect forcing owing to the sulfate aerosol change plays a minor role in modulating the thermal response in the model. In this work, we did not separate the direct and indirect effects of sulfate aerosols on the EASM. However, explicit understanding of each aerosol effect is critical to include the roles of aerosols in climate variability in global models. We plan to address this issue with improved models in the near future.

Strong cooling at 25°N–35°N in the low troposphere acts to change the meridional temperature gradient in eastern China. Concurrently, a weakening in the temperature gradient in eastern China results in a decelerating jet stream, as shown in Figure 4b, which displays the differences in zonal and meridional circulations averaged over the 100°E–140°E between the two periods in the SO₂ run. Our analysis of the results from the SO₂ run reveals that the radiative cooling owing to the enhancement of sulfate aerosol decelerates the upper level jet stream at the jet exit region, as indicated by the negative upper level zonal wind anomaly at 35–45°N. This jet weakening induces secondary circulation with rising motion around 18–23°N and sinking motion around 35–40°N and causes an increase in precipitation around 18–23°N, resulting in a slight increase of EASM intensity (Figure 4c).

According to the previous study [Jacobson and Kaufman, 2006], aerosol forcing can cause the SST cooling with the reduction of wind speeds by stabilizing air, which is consistent with a reduction in wind speed over land in China (Figure 4b). Subsequently, a reduction of wind speed is able to cause less water evaporation over the ocean, contributing to the weakening of the EASM [Jacobson and Kaufman, 2006]. The SO₂ run does not consider the feedback process between sulfate aerosol forcing and SST; therefore, we cannot exclude the possibility that the intensity of EASM in the SO₂ run would be changed by allowing SST-ocean interactions. However, it is found that the difference in 2 m air temperature between the two periods (2001–2010 minus 1985–1994) in the SO₂ run is small over the ocean (Figure S6 in the supporting information). This indicates that the effect of SST changes due to sulfate aerosol forcing might be small, which may be due to a very short lifetime of sulfate aerosol in ambient atmosphere around 3–5 days [Park et al., 2004].

4. Summary

To examine the effects of sulfate aerosol forcing on the EASM, we conducted three sets of CAM5 model experiments including control run, SST run, and SO₂ run. Each set of experiments was performed with four ensemble members, the average of which was compared with the observations. The model reasonably captured the general patterns of precipitation and low-level winds over East Asia during JJA, although it failed to reproduce the detailed precipitation structures, reflecting the deficiency of the present global models.

Our analysis of the EASM index based on the observations showed that the intensity of the EASM has decreased over the past few decades, which is consistent with the previous studies [Yu et al., 2004; Wang et al., 2009]. We found that both the control run and the SST run reproduced such a weakening of the EASM. In contrast, the model with anthropogenic sulfate forcing showed a slight increasing trend of the EASM index, indicating that SST forcing has resulted in the weakening of the EASM, while the effect of regional sulfate aerosol forcing acts to strengthen the EASM for 1985–2010. The weakening of the EASM due to SST forcings is mainly associated with the weakening of meridional temperature gradient for 2001–2010 along with the southward shift of the jet stream. This results in a downward motion at the right exit of the jet, causing a decrease in precipitation around 20°N. On the other hand, the effect of sulfate aerosol forcing causes a cooling in southeastern China, which results in the weakening of the meridional temperature gradient in eastern China. As a result, the upper level jet stream decelerates at the jet exit region with the rising motion in southeastern. Consequently, an increase in precipitation around 18–23°N is induced by the effect of sulfate aerosol forcing over East Asia.

Acknowledgments

This study was funded by the Korea Ministry of Environment (MOE) as "Climate Change Correspondence Program" and by the GEMS Program of MOE. The National Center for Environmental Prediction (NCEP) and National Center for Atmospheric Research (NCAR) global reanalysis atmospheric variables can also be obtained from Earth System Research Laboratory (<http://www.eri.noaa.gov/psd/data/gridded/data.ncep.reanalysis.html>). The Global Precipitation Climatology Project (GPCP) monthly precipitation data set version 2.2 can be obtained from <http://www.esrl.noaa.gov/psd/data/gridded/data.gpcp.html>. The monsoon index can be obtained from http://www.cpc.ncep.noaa.gov/products/Global_Monsoons/Asian_Monsoons/monsoon_index.shtml.

References

- Adler, R. F., et al. (2003), The version-2 Global Precipitation Climatology Project (GPCP) monthly precipitation analysis (1979–present), *J. Hydrometeorol.*, *4*, 1147–1167, doi:10.1175/1525-7541.
- Albrecht, B. A. (1989), Aerosols, cloud microphysics, and fractional cloudiness, *Science*, *245*, 1227–1230, doi:10.1126/science.245.4923.1227.
- Bollasina, M. A., Y. Ming, and V. Ramaswamy (2011), Anthropogenic aerosols and the weakening of the South Asian summer monsoon, *Science*, *334*, 502–505, doi:10.1126/science.1204994.
- Bollasina, M. A., Y. Ming, and V. Ramaswamy (2013), Earlier onset of the Indian monsoon in the late twentieth century: The role of anthropogenic aerosols, *Geophys. Res. Lett.*, *40*, 3715–3720, doi:10.1002/grl.50719.
- Bollasina, M. A., Y. Ming, V. Ramaswamy, M. D. Schwarzkopf, and V. Naik (2014), Contribution of local and remote anthropogenic aerosols to the twentieth century weakening of the South Asian Monsoon, *Geophys. Res. Lett.*, *41*, 680–687, doi:10.1002/2013GL058183.
- Cowan, T., and W. Cai (2011), The impact of Asian and non-Asian anthropogenic aerosols on 20th century Asian summer monsoon, *Geophys. Res. Lett.*, *38*, L11703, doi:10.1029/2011GL047268.
- Ganguly, D., P. J. Rasch, H. Wang, and J.-H. Yoon (2012), Climate response of the South Asian monsoon system to anthropogenic aerosols, *J. Geophys. Res.*, *117*, D13209, doi:10.1029/2012JD017508.
- Guo, L., E. J. Highwood, L. C. Shaffrey, and A. G. Turner (2013), The effect of regional changes in anthropogenic aerosols on rainfall of the East Asian summer monsoon, *Atmos. Chem. Phys.*, *13*, 1521–1534, doi:10.5194/acp-13-1521-2013.
- Guo, L., A. G. Turner, and E. J. Highwood (2015), Impacts of 20th century aerosol emissions on the South Asian monsoon in the CMIP5 models, *Atmos. Chem. Phys.*, *15*(11), 6367–6378, doi:10.5194/acp-15-6367-2015.
- Haywood, J., and O. Boucher (2000), Estimates of the direct and indirect radiative forcing due to tropospheric aerosols: A review, *Rev. Geophys.*, *38*, 513–543, doi:10.1029/1999RG000078.
- Jacobson, M. Z., and Y. J. Kaufman (2006), Wind reduction by aerosol particles, *Geophys. Res. Lett.*, *33*, L24814, doi:10.1029/2006GL027838.
- Jiang, Y., X. Liu, X.-Q. Yang, and M. Wang (2013), A numerical study of the effect of different aerosol types on East Asian summer clouds and precipitation, *Atmos. Environ.*, *70*, 51–63, doi:10.1016/j.atmosenv.2012.12.039.
- Kanamitsu, M., W. Ebisuzaki, J. Woollen, S.-K. Yang, J. J. Hnilo, M. Fiorino, and G. L. Potter (2002), NCEP-DOE AMIP-II Reanalysis (R-2), *Bull. Am. Meteorol. Soc.*, *83*(11), 1631–1643, doi:10.1175/BAMS-83-11-1631.
- Kim, M.-K., W. K. M. Lau, K.-M. Kim, and W.-S. Lee (2007), A GCM study of effects of radiative forcing of sulfate aerosol on large scale circulation and rainfall in East Asia during boreal spring, *Geophys. Res. Lett.*, *34*, L24701, doi:10.1029/2007GL031683.
- Kuhlmann, J., and J. Quaas (2010), How can aerosols affect the Asian summer monsoon? Assessment during three consecutive pre-monsoon seasons from CALIPSO satellite data, *Atmos. Chem. Phys.*, *10*, 4673–4688, doi:10.5194/acp-10-4673-2010.
- Li, J., and Q. Zeng (2002), A unified monsoon index, *Geophys. Res. Lett.*, *29*(8), 1274, doi:10.1029/2001GL013874.
- Li, J., Z. Han, and Z. Xie (2013), Model analysis of long-term trends of aerosol burdens and direct radiative forcings over East Asia, *Tellus*, *65B*, 20410, doi:10.3402/tellusb.v65i0.20410.
- Liu, X., et al. (2012), Toward a minimal representation of aerosols in climate models: description and evaluation in the Community Atmosphere Model CAM5, *Geosci. Model Dev.*, *5*, 709–739, doi:10.5194/gmd-5-709-2012.
- Liu, Y. U., J. Sun, and B. A. I. Yang (2009), The effects of black carbon and sulphate aerosols in China regions on East Asia monsoons, *Tellus*, *61B*, 642–656, doi:10.1111/j.1600-0889.2009.00427.x.
- Nan, S., and J. Li (2003), The relationship between the summer precipitation in the Yangtze River valley and the boreal spring Southern Hemisphere annular mode, *Geophys. Res. Lett.*, *30*(24), 2266, doi:10.1029/2003GL018381.
- Neale, R. B., et al. (2012), NCAR Tech. Note NCAR/TN-486+STR, National Center for Atmospheric Research, 268 pp., Boulder, Colo.
- Ohara, T., H. Akimoto, J. Kurokawa, N. Horii, K. Yamaji, X. Yan, and T. Hayasaka (2007), An Asian emission inventory of anthropogenic emission sources for the period 1980–2020, *Atmos. Chem. Phys.*, *7*, 4419–4444, doi:10.5194/acp-7-4419-2007.
- Park, R. J., D. J. Jacob, B. D. Field, R. M. Yantosca, and M. Chin (2004), Natural and transboundary pollution influences on sulfate-nitrate-ammonium aerosols in the United States: Implications for policy, *J. Geophys. Res.*, *109*, D15204, doi:10.1029/2003JD004473.
- Rayner, N. A., D. E. Parker, E. B. Horton, C. K. Folland, L. V. Alexander, D. P. Rowell, E. C. Kent, and A. Kaplan (2003), Global analyses of sea surface temperature, sea ice, and night marine air temperature since the late nineteenth century, *J. Geophys. Res.*, *108*(14), 4407, doi:10.1029/2002JD002670.
- Shi, N., and Q. Zhu (1996), An abrupt change in the intensity of the East Asian summer monsoon index and its relationship with temperature and precipitation over east China, *Int. J. Climatol.*, *16*, 757–764, doi:10.1002/(SICI)1097-0088.
- Smith, S. J., J. V. Aardenne, Z. Klimont, R. J. Andres, A. Volke, and A. S. Delgado (2011), Anthropogenic sulfur dioxide emissions: 1850–2005, *Atmos. Chem. Phys.*, *11*, 1101–1116, doi:10.5194/acp-11-1101-2011.
- Sperber, K. R., H. Annamalai, I. S. Kang, A. Kitoh, A. Moise, A. Turner, B. Wang, and T. Zhou (2013), The Asian summer monsoon: An intercomparison of CMIP5 vs. CMIP3 simulations of the late 20th century, *Clim. Dyn.*, *41*, 2711–2744, doi:10.1007/s00382-012-1607-6.
- Streets, D. G., et al. (2003), An inventory of gaseous and primary aerosol emissions in Asia in the year 2000, *J. Geophys. Res.*, *108*(D21), 8809, doi:10.1029/2002JD003093.
- Trenberth, K. E., D. P. Stepaniak, and J. M. Caron (2000), The global monsoon as seen through the divergent atmospheric circulation, *J. Clim.*, *13*, 3969–3993, doi:10.1175/1520-0442.
- Turner, A. G., and H. Annamalai (2012), Climate change and the South Asian summer monsoon, *Nat. Clim. Change*, *2*, 587–595, doi:10.1038/nclimate1495.
- Twomey, S. (1977), The influence of pollution on the shortwave albedo of clouds, *J. Atmos. Sci.*, *34*, 1149–1152, doi:10.1175/1520-0469(1977)034<1149:TIOPOT>2.0.CO;2.
- Wang, B., and Q. Ding (2006), Changes in global monsoon precipitation over the past 56 years, *Geophys. Res. Lett.*, *33*, L06711, doi:10.1029/2005GL025347.
- Wang, B., R. Wu, and K. M. Lau (2001), Interannual variability of the Asian summer monsoon: Contrasts between the Indian and the Western North Pacific–East Asian monsoons, *J. Clim.*, *14*, 4073–4090, doi:10.1175/1520-0442.
- Wang, B., Y. Z. LinHo, and M. M. Lu (2004), Definition of South China Sea monsoon onset and commencement of the East Asia summer monsoon, *J. Clim.*, *17*, 699–710, doi:10.1175/2932.1.
- Wang, B., Z. Wu, J. Li, J. Liu, C.-P. Chang, Y. Ding, and G. Wu (2008), How to measure the strength of the East Asian summer monsoon, *J. Clim.*, *21*, 4449–4463, doi:10.1175/2008JCLI2183.1.

- Wang, B., F. Huang, Z. Wu, J. Yang, X. Fu, and K. Kikuchi (2009), Multi-scale climate variability of the South China Sea monsoon: A review, *Dyn. Atmos. Oceans*, 47, 15–37, doi:10.1016/j.dynatmoce.2008.09.004.
- Yu, R., B. Wang, and T. Zhou (2004), Tropospheric cooling and summer monsoon weakening trend over East Asia, *Geophys. Res. Lett.*, 31, L22212, doi:10.1029/2004GL021270.
- Zhu, C., W.-S. Lee, H. Kang, and C.-K. Park (2005), A proper monsoon index for seasonal and interannual variations of the East Asian monsoon, *Geophys. Res. Lett.*, 32, L02811, doi:10.1029/2004GL021295.
- Zhu, J., H. Liao, and J. Li (2012), Increases in aerosol concentrations over eastern China due to the decadal-scale weakening of the East Asian summer monsoon, *Geophys. Res. Lett.*, 39, L09809, doi:10.1029/2012GL051428.